mathematics

MDPI

Article

Modified Exp-Function Method to Find Exact Solutions of Ionic Currents along Microtubules

Attaullah [1,†], Muhammad Shakeel [1], Nehad Ali Shah [2,*,†] and Jae Dong Chung [2]

[1] Department of Mathematics, University of Wah, Wah Cantonment, Punjab 47040, Pakistan; attaullahsial275@gmail.com (A.); muhammad.shakeel@uow.edu.pk (M.S.)
[2] Department of Mechanical Engineering, Sejong University, Seoul 05006, Korea; jdchung@sejong.ac.kr
* Correspondence: nehadali199@yahoo.com or nehadali199@sejong.ac.kr
† These authors contributed equally to this work.

Abstract: A number of solitary wave solutions for microtubules (MTs) are observed in this article by using the modified exp-function approach. We tackle the problem by treating the results as nonlinear RLC transmission lines, and then finding exact solutions to Nonlinear Evolution Equation (NLEE) containing parameters of particular importance in biophysics and nanobiosciences. For this equation, we find trigonometric, hyperbolic, rational, and exponential function solutions, as well as soliton-like pulse solutions. A comparison with other approach indicates the legitimacy of the approach we devised as well as the fact that our method offers extra solutions. Finally, we plot 2D, 3D and contour visualizations of the exact results that we observed using our approach using appropriate parameter values with the help of software Mathematica 10.

Keywords: exact solutions; nonlinear RLC transmission lines; analytical method; nonlinear evolution equation of microtubules

MSC: 83C15; 35A20; 35C05; 35C07; 35C08

check for updates

Citation: Attaullah; Shakeel, M.; Shah, N.A.; Chung, J.D. Modified Exp-Function Method to Find Exact Solutions of Ionic Currents along Microtubules. *Mathematics* **2022**, *10*, 851. https://doi.org/10.3390/math10060851

Academic Editors: Mingheng Li, Hui Sun and Yang Liu

Received: 21 January 2022
Accepted: 4 March 2022
Published: 8 March 2022

1. Introduction

Various fields of applied mathematics, engineering and mathematical physics, such as hydrodynamics, solid state physics, fiber optics, biology, fluid mechanics, plasma physics, geochemistry, and chemical systems confront multiple technical challenges in developing an understanding of nonlinear phenomena. Calculating numerical and analytical solutions of nonlinear evolution equations (NLEEs), notably solitary and travelling wave solutions, is crucial in soliton theory [1]. Recently, symbolic software such as Maple, Mathematica, and Matlab have been popular for determining numerical solutions, exact solutions, and analytical solutions to NLEEs. These systems make difficult and laborious algebraic computations easier.

Numerous powerful methods have been developed for finding exact travelling wave and solitary wave solutions of the nonlinear evolution equations, such as, rational perturbation method [2], Painlevé expansion method [3], Hirota's bilinear method [4], the (G'/G)-expansion method [5,6], F-expansion method [7], Jacobi elliptic function method [8–10], the Homogeneous Balance method [11], the extended Tanh-function method [12], modified Tanh-function method [13–17], $\exp(-\phi(\xi))$-expansion method [18], and the direct method [19].

Microtubules (MTs) are nanotube-shaped cytoskeleton biopolymers that are required for intracellular trafficking, division, cell motility, and information processing in neural processes. Higher neuronal processes, including as memory and the formation of consciousness, have also been linked to MTs. However, it is currently uncertain how MTs handle and process electrical data. Based on polyelectrolyte characteristics of cylindrical biopolymers, we develop a new model for ionic waves along MTs in this paper. Each microtubule duplex protein is a capacitive, resistive, and negative incrementally resistive electric element [20]. The role of nanopores (NPs) that exist between neighboring duplex within an MT wall, which exhibits features comparable to ionic channels, was highlighted in [21,22]. The behaviour of MTs as biomolecular transistors capable of magnifying electrical information in neurons might be explained using these NPs. The origin and the derivation's physical characteristics of the following equation relating to the ionic currents are presented in [23].

$$R_2 C_0 L^2 u_{xxt} + L^2 u_{xx} + 2R_1 C_0 \delta\, u u_t - R_1 C_0\, u_t = 0, \tag{1}$$

where $R_1 = 10^9\ \Omega$ and $R_2 = 7 \times 10^6\ \Omega$ represent transverse and longitudinal components of the resistance of an elementary ring (ER). Also, the parameter $\delta\ \ (\delta < 1)$ elucidates the nonlinearity to an ER capacitor in microtubules. In this case, $L = 8 \times 10^{-9}$ m, while $C_0 = 1.8 \times 10^{-15}$ F being the ER's overall maximal capacitance. Using the modified extended tanh function approach, Sekulic et al. [13] analyzed the equation of MTs as a nonlinear RLC transmission line to get solitary wave solutions. The improved generalized Riccati equation mapping method was used by Zayed et al. [24] to solve a nonlinear partial differential equation representing the dynamics of ionic currents along microtubules and construct travelling wave solutions.

The goal of this research is to use the modified exp-function approach to find new exact solutions to nonlinear PDEs of particular relevance in nanobiosciences, such as transmission line model of nanoionic currents along microtubules, which play a vital role in cell signaling. Comparison of the newly obtained solutions with the existing solutions in the literature is given in the form of the table which shows that our solutions are new and more general.

2. The Description of the Method

In this part of the research article, we will momentarily present the main steps of the proposed modified exp-function method [25]. Consider a general NLPDE of the form

$$T(U,\ U_x,\ U_t,\ U_{xx},\ U_{tt}, U_{tx}\ \ldots) = 0, \tag{2}$$

where T is polynomial in $U(x,t)$ and its partial derivatives, which contains the nonlinear terms and higher order derivatives, and $U = U(x,t)$ is an unrevealed function. The main steps of this method are:

Step 1: The following change of variable,

$$U(x,t) = u(\theta), \qquad \theta = \frac{x}{L} - \frac{c}{\tau}t\,, \tag{3}$$

where $\tau = R_1 C_0 = 1.32 \times 10^{-6}\ s$, and c is the non-dimensional wave velocity, converts Equation (2) into a nonlinear ordinary differential equation:

$$R\big(u,\ u',\ u'',\ u''',\ \ldots\big) = 0, \tag{4}$$

where the superscripts indicate the ordinary derivatives with regard to θ, while R is a polynomial of u and its derivatives.

Step 2: Assume that the travelling wave solution of Equation (4) can be expressed as follows:

$$u(\theta) = \frac{\sum_{i=0}^{M} A_i[\exp(-\Phi(\theta))]^i}{\sum_{j=0}^{N} B_j[\exp(-\Phi(\theta))]^j} = \frac{A_0 + A_1 \exp\left(-\Phi(\theta)\right) + \ldots + A_M \exp\left(M(-\Phi(\theta))\right)}{B_0 + B_1 \exp\left(-\Phi(\theta)\right) + \ldots + B_N \exp\left(N(-\Phi(\theta))\right)}, \tag{5}$$

where A_i, B_j, $(0 \le i \le M\ ,\ 0 \le j \le N)$ are the constants to be calculated later, such that $A_M \ne 0$, $B_N \ne 0$, and also $\Phi = \Phi(\theta)$ satisfies the following ordinary differential equation (ODE);

$$\Phi'(\theta) = \exp(-\Phi(\theta)) + a\ \exp(\Phi(\theta)) + b. \tag{6}$$

Equation (6) has the following solution sets:
a: When $a \neq 0,\ b^2 - 4a > 0$,

$$\Phi(\theta) = ln\left(\frac{-\sqrt{b^2 - 4a}}{2a}\tanh\left(\frac{\sqrt{b^2 - 4a}}{2}(\theta + E)\right) - \frac{b}{2a}\right). \tag{7}$$

b: When $a \neq 0,\ b^2 - 4a < 0$,

$$\Phi(\theta) = ln\left(\frac{\sqrt{-b^2 + 4a}}{2a}\tan\left(\frac{\sqrt{-b^2 + 4a}}{2}(\theta + E)\right) - \frac{b}{2a}\right). \tag{8}$$

c: When $a = 0, b \neq 0,\ b^2 - 4a > 0$,

$$\Phi(\theta) = -\ ln\left(-\frac{b}{\exp(b(\theta + E)) - 1}\right). \tag{9}$$

d: When $a \neq 0, b \neq 0,\ b^2 - 4a = 0$,

$$\Phi(\theta) = ln\left(-\frac{2b(\theta + E) + 4}{b^2(\theta + E)}\right). \tag{10}$$

e: When $a = 0, b = 0,\ b^2 - 4a = 0$,

$$\Phi(\theta) = ln(\theta + E). \tag{11}$$

such that $A_{0,}\ A_{1,}\ A_{2,} \dots\ A_{M,}\ B_{0,}\ B_{1,}\ B_{2,} \dots\ B_{N,}\ E,\ a,\ b$ are the constants to be calculated later. By using the homogeneous balance principle between the highest order nonlinear term and highest order linear term occurring in Equation (5), we can find the positive integers M and N.

Step 3: Substituting the Equations (6)–(11) into Equation (5), we get a polynomial in different powers of the exp $(-\Phi(\theta))$ and equating all coefficients to zero, yields a system of algebraic equations which can be solved to find $A_0,\ A_1,\ A_2, \dots\ A_M,\ B_0,\ B_1,\ B_2, \dots\ B_N,\ E,\ a,\ b$ by using Maple 18. Substituting the values of $A_0,\ A_1,\ A_2, \dots\ A_M,\ B_0,\ B_1,\ B_2, \dots\ B_N,\ E,\ a,\ b$ in the Equation (5), the general solutions of the Equation (5) complete the fortitude of the solution of Equation (1).

Remark 1. *If we put $B_0 = 1$, $B_1 = 0$, and $A_3 = 0$, then our solution (14) coincides with the trial solution (14) of Alam and Alam [18].*

3. Applications

This section discusses the use of the modified exp-function method to obtain new analytical solutions for nonlinear RLC transmission lines such as a new hyperbolic function solution and a complex function solution. The travelling wave variable Equation (4) converts Equation (1) into the following NLODE:

$$U''(\theta) - \frac{\alpha_1}{c}\left(U'(\theta)\right) + \frac{\alpha_2 U(\theta)^2}{2} - \alpha_3 U(\theta) = 0, \tag{12}$$

where $\alpha_1 = \frac{\tau}{R_2 C_0}$, $\alpha_2 = \frac{2R_1\delta}{R_2}$, $\alpha_3 = \frac{R_1}{R_2}$.

The following equation is derived using the balance principle to determine the link between U^2 and U'':

$$M = N + 2. \tag{13}$$

We can obtain several new analytical solutions for Equation (1) utilizing this relationship, as follows:

Let us say $N = 1$ and $M = 3$, and we will be able to write:

$$\mathrm{U} = \frac{A_0 + A_1 \exp(-\Phi) + A_2 \exp(2(-\Phi)) + A_3 \exp(3(-\Phi))}{B_0 + B_1 \exp(-\Phi)}, \tag{14}$$

such that $A_3 \neq 0$ and $B_1 \neq 0$. Substituting Equation (14) along with Equation (6) into Equation (12), we obtain a polynomial including $\exp\left(-\Phi(\theta)\right)$ and its numerous powers. Consequently, we have a system of algebraic equations from the coefficients of polynomial of $\exp(-\Phi(\theta))$. After solving this system with Maple 18, we get the following values for the coefficients:

Case 1:

$$\begin{aligned} &b = \tfrac{1}{6}\sqrt{144a - 6\alpha_3}\ ,\ c = \tfrac{I}{5}\tfrac{\sqrt{6}\alpha_1}{\sqrt{\alpha_3}}\ ,\ A_0 = \tfrac{B_0\left(I\sqrt{144a-6\alpha_3}\sqrt{6\alpha_3}-72a+6\alpha_3\right)}{6\alpha_2}, \\ &A_1 = -\tfrac{1}{\alpha_2}\left(\tfrac{B_1\alpha_3\sqrt{144a-6\alpha_3}}{\sqrt{-6\alpha_3}} + \tfrac{12B_0\alpha_3}{\sqrt{-6\alpha_3}} + 2B_0\sqrt{144a - 6\alpha_3} + 12aB_1 - B_1\alpha_3\right), \\ &A_2 = \tfrac{1}{\alpha_2}\left(2B_1\sqrt{-6\alpha_3} - 2B_1\sqrt{144a - 6\alpha_3} - 12B_0\right)\ ,\ A_3 = -\tfrac{12B_1}{\alpha_2}\ . \end{aligned} \tag{15}$$

Case 2:

$$\begin{aligned} &a = \tfrac{1}{4}b^2 - \tfrac{1}{24}\alpha_3\ ,\ c = \tfrac{1}{5}\tfrac{\sqrt{6}\ \alpha_1}{\sqrt{\alpha_3}}\ ,\ A_0 = -\tfrac{1}{2}\tfrac{\left(2b\sqrt{\alpha_3}+\sqrt{6}\ \left(b^2-\frac{1}{12}\alpha_3\right)\right)B_0\sqrt{6}}{\alpha_2},\ A_3 = -\tfrac{12B_1}{\alpha_2} \\ &A_1 = \tfrac{1}{2}\tfrac{-2\sqrt{6}\ (bB_1+2B_0)\sqrt{\alpha_3}+\left(-6b^2+3\alpha_3\right)B_1-24bB_0}{\alpha_2}\ ,\ A_2 = -\tfrac{2\left(B_1\sqrt{\alpha_3}+(bB_1+B_0)\sqrt{6}\right)\sqrt{6}}{\alpha_2}\ . \end{aligned} \tag{16}$$

Substituting Equations (7)–(11) along with the value of the coefficients from Equation (15) into Equation (14), we obtained the following travelling wave solutions for Equation (1), as follows:

When $a \neq 0,\ b^2 - 4a > 0$,

$$\begin{aligned} U_1(x,t) = &\frac{1}{B_0 - \frac{B_1}{\frac{\sqrt{b^2-4a}\tanh\left(\frac{1}{2}\sqrt{b^2-4a}(\theta+E)\right)}{2a}+\frac{b}{2a}}}\left(A_0 - \frac{A_1}{\frac{\sqrt{b^2-4a}\tanh\left(\frac{1}{2}\sqrt{b^2-4a}(\theta+E)\right)}{2a}+\frac{b}{2a}}\right. \\ &\left.-\frac{A_2}{\left(\frac{\sqrt{b^2-4a}\tanh\left(\frac{1}{2}\sqrt{b^2-4a}(\theta+E)\right)}{2a}+\frac{b}{2a}\right)^2} - \frac{A_3}{\left(\frac{\sqrt{b^2-4a}\tanh\left(\frac{1}{2}\sqrt{b^2-4a}(\theta+E)\right)}{2a}+\frac{b}{2a}\right)^3}\right), \end{aligned} \tag{17}$$

When $a \neq 0,\ b^2 - 4a < 0$,

$$\begin{aligned} U_2(x,t) = &\frac{1}{B_0 + \frac{B_1}{\frac{1}{2}\frac{\sqrt{-b^2+4a}\tan\left(\frac{1}{2}\sqrt{-b^2+4a}(\theta+E)\right)}{a}-\frac{b}{2a}}}\left(A_0 + \frac{A_1}{\frac{1}{2}\frac{\sqrt{-b^2+4a}\tan\left(\frac{1}{2}\sqrt{-b^2+4a}(\theta+E)\right)}{a}-\frac{b}{2a}}\right. \\ &\left.+\frac{A_2}{\left(\frac{1}{2}\frac{\sqrt{-b^2+4a}\tan\left(\frac{1}{2}\sqrt{-b^2+4a}(\theta+E)\right)}{a}-\frac{b}{2a}\right)^2} + \frac{A_3}{\left(\frac{1}{2}\frac{\sqrt{-b^2+4a}\tan\left(\frac{1}{2}\sqrt{-b^2+4a}(\theta+E)\right)}{a}-\frac{b}{2a}\right)^3}\right), \end{aligned} \tag{18}$$

When $a = 0, b \neq 0,\ b^2 - 4a > 0$,

$$U_3(x,t) = \frac{1}{B_0 + \frac{B_1 b}{e^{b(\theta+E)}-1}}\left(A_0\left(\frac{b}{e^{b(\theta+E)}-1}\right) + A_1\left(\frac{b}{e^{b(\theta+E)}-1}\right) + A_2\left(\frac{b}{e^{b(\theta+E)}-1}\right)^2 + A_3\left(\frac{b}{e^{b(\theta+E)}-1}\right)^3\right), \tag{19}$$

When $a \neq 0,\ b \neq 0,\ b^2 - 4a = 0$,

$$U_4(x,t) = \frac{1}{B_0 - \frac{B_1 b^2(\theta+E)}{2b(\theta+E)+4}}\left(A_0 - \frac{A_1\, b^2(\theta+E)}{2b(\theta+E)+4} + \frac{A_2\, b^2(\theta+E)^2}{(2b(\theta+E)+4)^2} - \frac{A_3\, b^2(\theta+E)^3}{(2b(\theta+E)+4)^3}\right) \tag{20}$$

When $a = 0, b = 0,\ b^2 - 4a = 0$,

$$U_5(x,t) = \frac{\theta^3 A_0 + (3\,E\,A_0 + A_1)\,\theta^2 + \left(3E^2 A_0 + 3\,E\,A_1 + A_2\right)\theta + E^3 A_0 + E^2 A_1 + E A_2 + A_3}{(E\,B_0 + \theta\,B_0 + B_1)(\theta + E)^2}, \tag{21}$$

where $\theta = \frac{x}{L} - \frac{c}{\tau}t$ and the value of coefficients $A_0,\ A_1,\ A_2, A_3,\ b,$ and c are given in Equation (15).

Similarly, substituting Equations (7)–(11) along with the value of the coefficients from Equation (16) into Equation (14), we obtained the following travelling wave solutions for Equation (1):

When $a \neq 0,\ b^2 - 4a > 0$,

$$\begin{aligned} U_6(x,t) = {} & \frac{1}{B_0 + \frac{B_1}{-\frac{1}{2}\frac{\sqrt{b^2-4a}\tanh\left(\frac{1}{2}\sqrt{b^2-4a}(\theta+E)\right)}{a} - \frac{b}{2a}}}\Bigg(A_0 + \frac{A_1}{-\frac{1}{2}\frac{\sqrt{b^2-4a}\tanh\left(\frac{1}{2}\sqrt{b^2-4a}(\theta+E)\right)}{a} - \frac{b}{2a}} \\ & + \frac{A_2}{\left(-\frac{1}{2}\frac{\sqrt{b^2-4a}\tanh\left(\frac{1}{2}\sqrt{b^2-4a}(\theta+E)\right)}{a} - \frac{b}{2a}\right)^2} + \frac{A_3}{\left(-\frac{1}{2}\frac{\sqrt{b^2-4a}\tanh\left(\frac{1}{2}\sqrt{b^2-4a}(\theta+E)\right)}{a} - \frac{b}{2a}\right)^3}\Bigg), \end{aligned} \tag{22}$$

When $a \neq 0,\ b^2 - 4a < 0$,

$$\begin{aligned} U_7(x,t) = {} & \frac{1}{B_0 + \frac{B_1}{\frac{1}{2}\frac{\sqrt{-b^2+4a}\tan\left(\frac{1}{2}\sqrt{-b^2+4a}(\theta+E)\right)}{a} - \frac{b}{2a}}}\Bigg(A_0 + \frac{A_1}{\frac{1}{2}\frac{\sqrt{-b^2+4a}\tan\left(\frac{1}{2}\sqrt{-b^2+4a}(\theta+E)\right)}{a} - \frac{b}{2a}} \\ & + \frac{A_2}{\left(\frac{1}{2}\frac{\sqrt{-b^2+4a}\tan\left(\frac{1}{2}\sqrt{-b^2+4a}(\theta+E)\right)}{a} - \frac{b}{2a}\right)^2} + \frac{A_3}{\left(\frac{1}{2}\frac{\sqrt{-b^2+4a}\tan\left(\frac{1}{2}\sqrt{-b^2+4a}(\theta+E)\right)}{a} - \frac{b}{2a}\right)^3}\Bigg), \end{aligned} \tag{23}$$

When $a = 0, b \neq 0,\ b^2 - 4a > 0$,

$$U_8(x,t) = \frac{1}{B_0 + \frac{B_1 b}{e^{b(\theta+E)}-1}}\left(A_0\left(\frac{b}{e^{b(\theta+E)} - 1}\right) + A_1\left(\frac{b}{e^{b(\theta+E)} - 1}\right) + A_2\left(\frac{b}{e^{b(\theta+E)} - 1}\right)^2 + A_3\left(\frac{b}{e^{b(\theta+E)} - 1}\right)^3\right), \tag{24}$$

When $a \neq 0, b \neq 0,\ b^2 - 4a = 0$,

$$U_9(x,t) = \frac{1}{B_0 - \frac{B_1 b^2(\theta+E)}{2b(\theta+E)+4}}\left(A_0 - \frac{A_1 b^2(\theta+E)}{2b(\theta+E)+4} + \frac{A_2 b^2(\theta+E)^2}{(2b(\theta+E)+4)^2} - \frac{A_3 b^2(\theta+E)^3}{(2b(\theta+E)+4)^3}\right) \tag{25}$$

When $a = 0, b = 0,\ b^2 - 4a = 0$,

$$U_{10}(x,t) = \frac{\theta^3 A_0 + (3\,E\,A_0 + A_1)\,\theta^2 + \left(3E^2 A_0 + 3\,E\,A_1 + A_2\right)\theta + E^3 A_0 + E^2 A_1 + E A_2 + A_3}{(E\,B_0 + \theta\,B_0 + B_1)\,(\theta + E)^2}, \tag{26}$$

where $\theta = \frac{x}{L} - \frac{c}{\tau}t$ and the value of coefficients $A_0,\ A_1,\ A_2, A_3,\ a,$ and c are given in Equation (16).

4. Physical Expression of the Problem

The modified Exp-function method has been effectively used to solve nonlinear partial differential equation such as the nonlinear RLC transmission line model of nano-ionic currents along MTs in this paper. We have obtained new travelling wave solutions of the model of specific interest in biophysics using this method. Solitons, kink, singular kinks, and periodic solutions are among the solutions obtained. It's worth mentioning that the new solutions acquired using the modified Exp-function method validate the accuracy of the previous ones. The findings demonstrate that the modified Exp-function approach is a powerful mathematical tool that is both simple and concise, and that it may be used to solve other nonlinear evolution equations in physics. By selecting specific parameter values and charting the exact solutions generated using the mathematical software Mathematica 10, we examine the nature of numerous solutions obtained using the model of microtubules as nonlinear RLC transmission lines. Figures 1–8 illustrate the outcomes. Following these research results, we discovered that Equations (17)–(26) show kink, singular kink, solitons, singular solitons, and periodic solutions.

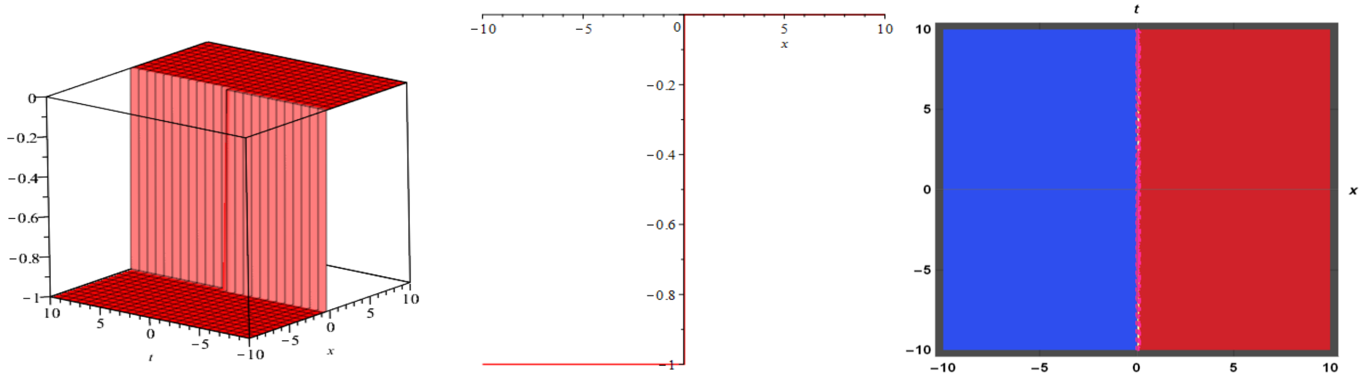

Figure 1. The solitary wave perspective view of the 3D, 2D, and contour plots of $U_1(x,t)$.

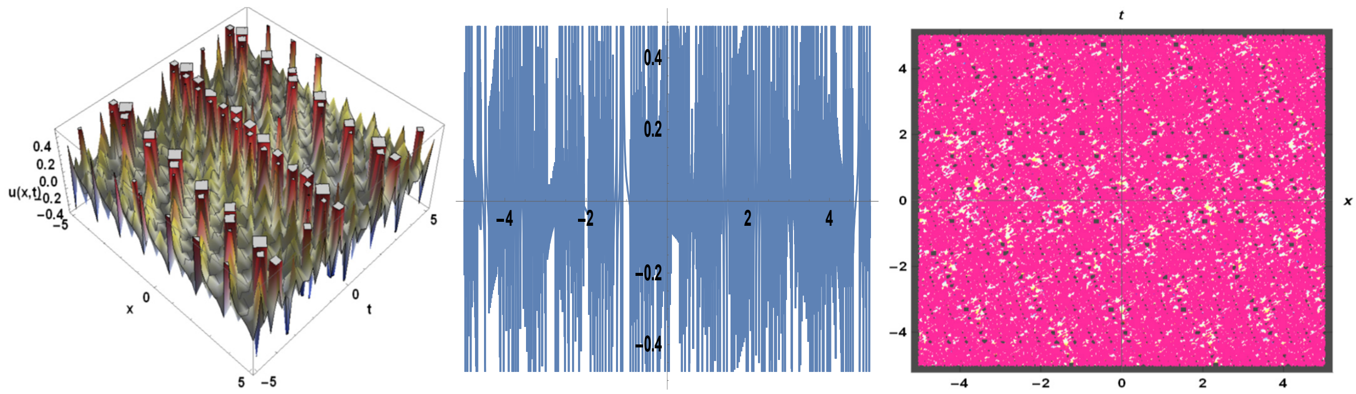

Figure 2. The solitary wave of perspective view of 3D, 2D, and contour plots of $U_2(x,t)$.

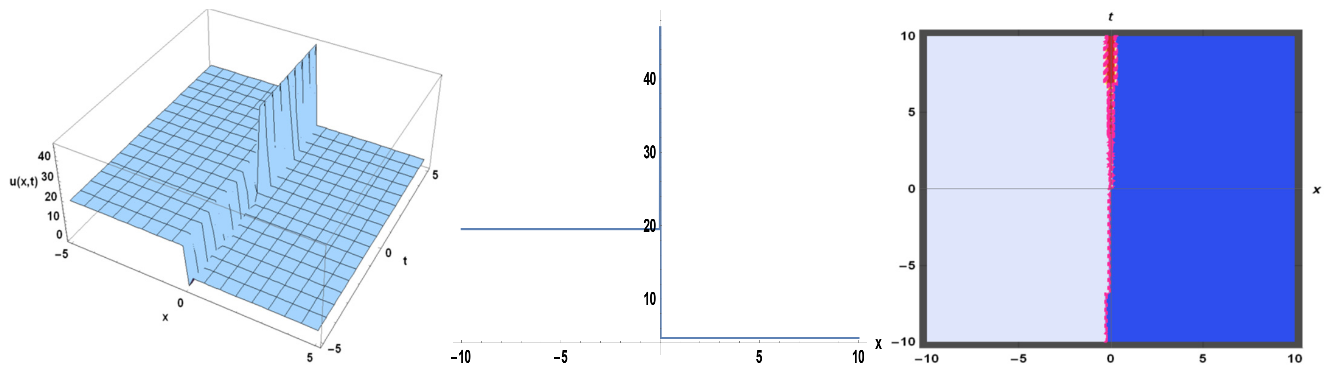

Figure 3. The solitary wave perspective view of the 3D, 2D, and contour plots of $U_3(x,t)$.

Graphical representations are a useful tool for discussing and articulating problem solutions in a clear and concise manner. A graph is a visual representation of quantitative or qualitative solutions or other data that is frequently compared. When performing computations, we need to have a fundamental comprehension of graphs. A kink wave is represented by Equation (17). Kink waves are waves that travel from one asymptotic state to the next. At infinity, the kink solutions approach a constant. Figure 1 pageants the shape of kink type exact solution for 3D, 2D, and contour plots of $U_1(x,t)$, for the unknown constants $R_1 = 10^9\ \Omega$, $R_2 = 10^6\ \Omega$, $C_0 = 1.8 \times 10^{-15}$ F, $L = 8 \times 10^{-9}$ m, a = 1, b = 3, E = 2, $B_0 = 2$, $B_1 = 1$, within the interval $-10 \leq x, t \leq 10$ for 3D graph and t = 1 for the 2D graph. Equation (18) represents the exact periodic travelling wave solution. Periodic wave solution is represented by Equation (18). Periodic wave solution is a travelling wave solution that is periodic in nature like $\cos(x-t)$. The 3D, 2D and contour plots for $U_2(x,t)$ are shown in Figure 2 for unknown parameters $R_1 = 10^9\ \Omega$, $R_2 = 10^6\ \Omega$, $C_0 = 1.8 \times 10^{-15}$ F, $L = 8 \times 10^{-9}$ m, $a = 1$, $b = 1$, $E = 1$, $B_0 = 2$, $B_1 = 1$, and within the interval $-5 \leq x, t \leq 5$ for the 3D graph and $t = 1$ for 2D graph. Figure 3 represents the 3D, 2D, and contour plots for singular kink type wave solution of $U_3(x,t)$ for parameters $R_1 = 10^9\ \Omega$, $R_2 = 10^6\ \Omega$, $C_0 = 1.8 \times 10^{-15}$ F, $L = 8 \times 10^{-9}$ m, $a = 0$, $b = 1$, $E = 5$, $B_0 = 2$, $B_1 = 1$, and within the interval $-5 \leq x, t \leq 5$ for the 3D graph and $t = 1$ for the 2D graph. Figure 4 displays the 3D, 2D, and contour plots for singular soliton type solution of $U_4(x,t)$ for $R_1 = 10^9\ \Omega$, $R_2 = 10^6\ \Omega$, $C_0 = 1.8 \times 10^{-15}$ F, $L = 8 \times 10^{-9}$ m, $a = 0$, $b = 1$, $E = 5$, $B_0 = 2$, $B_1 = 1$, and within the interval $-5 \leq x, t \leq 5$ for the 3D graph and $t = 1$ for the 2D graph. Figure 5 shows the 3D, 2D and contour plots of the rational function solution $U_5(x,t)$ that act like The bright multiple soliton solution for the unknown constants $R_1 = 10^9\ \Omega$, $R_2 = 10^6\ \Omega$, $C_0 = 1.8 \times 10^{-15}$ F, $L = 8 \times 10^{-9}$ m, $a = 0$, $b = 0$, $E = 2$, $B_0 = 1$, $B_1 = 2$, and within the interval $-15 \leq x, t \leq 15$ for the 3D graph and $t = 1$ for the 2D graph. The trigonometric function solution in Figure 6 demonstrates the periodic soliton solutions of $U_7(x,t)$ for the unknown constant $R_1 = 10^9\ \Omega$, $R_2 = 10^6\ \Omega$, $C_0 = 1.8 \times 10^{-15}$ F, $L = 8 \times 10^{-9}$ m, $a = 1$, $b = 1$, $E = 1$, $B_0 = 2$, $B_1 = 1$, to the interval, $-20 \leq x, t \leq 20$, for 3D graph and $t = 1$ for 2D graph. Figure 7 shows the exact travelling wave solution for $U_9(x,t)$ for unknown constants $R_1 = 10^9\ \Omega$, $R_2 = 10^6\ \Omega$, $C_0 = 1.8 \times 10^{-15}$ F, $L = 8 \times 10^{-9}$ m, $a = 1$, $b = 2$, $E = 5$, $B_0 = 2$, $B_1 = 1$, for 3D graph within the interval of $-10 \leq x, t \leq 10$ and $t = 1$ for 2D graph. Figure 8 represents the periodic trajectory of $U_{10}(x,t)$ for the known parameters $R_1 = 10^9\ \Omega$, $R_2 = 10^6\ \Omega$, $C_0 = 1.8 \times 10^{-15}$ F, $L = 8 \times 10^{-9}$ m, $a = 0$, $b = 0$, $E = 5$, $B_0 = 1$, $B_1 = 2$, for 3D graph and $t = 0.5$ for the 2D graph within the intervals $-1 \leq x \leq 1, 0 \leq t \leq 1$.

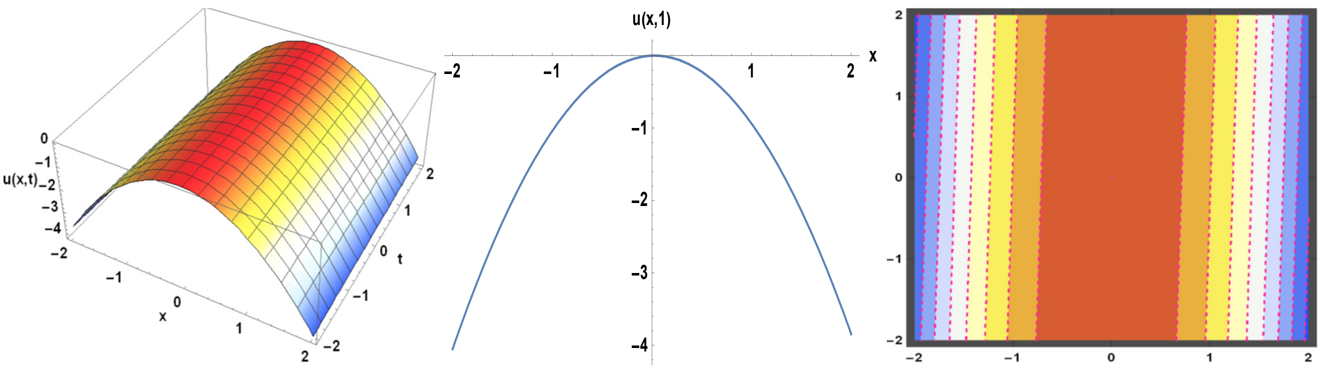

Figure 4. The solitary wave perspective view of the 3D, 2D, and contour plots of $U_4(x,t)$.

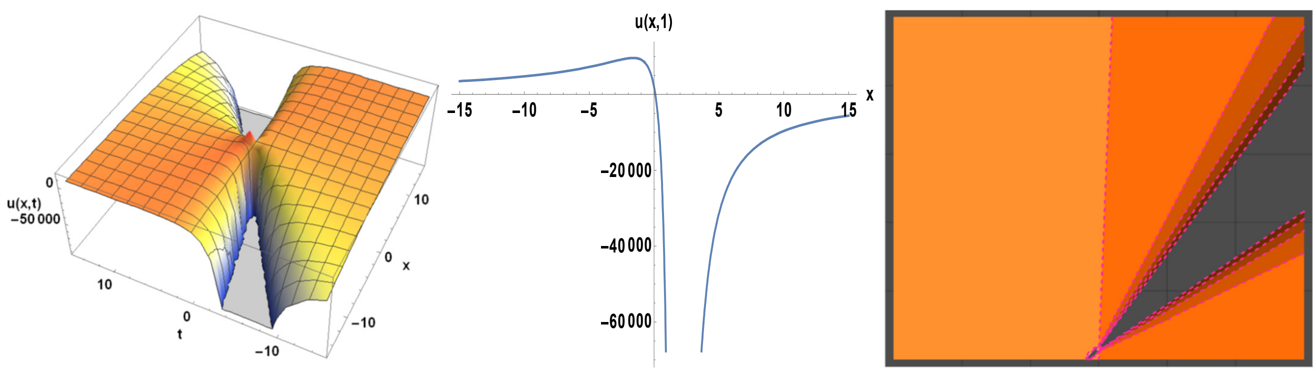

Figure 5. The solitary wave perspective view of the 3D, 2D, and contour plots of $U_5(x,t)$.

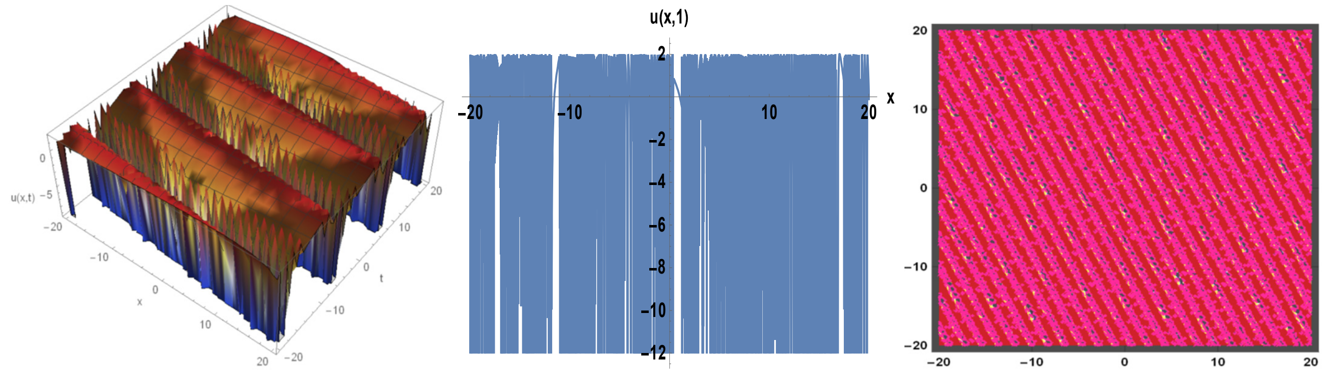

Figure 6. The solitary wave perspective view of the 3D, 2D and contour plots of $U_7(x,t)$.

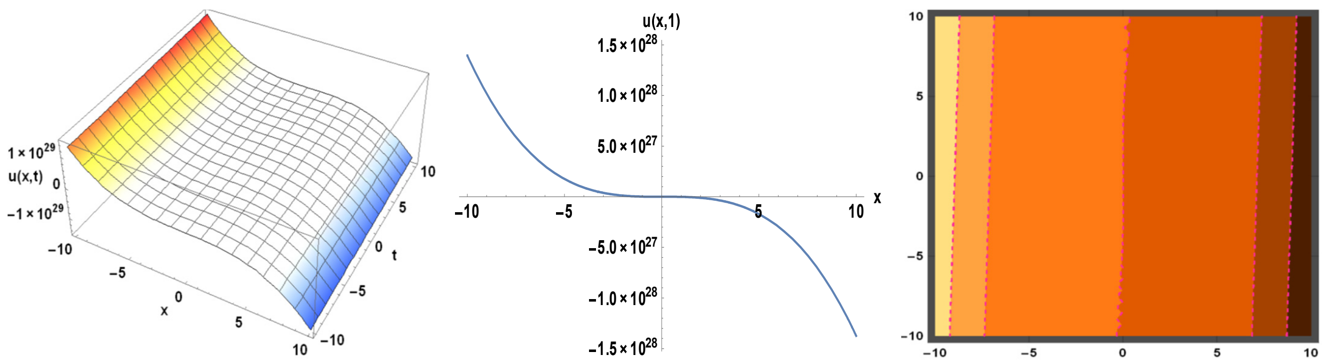

Figure 7. The solitary wave perspective view of the 3D, 2D and contour plots of $U_9(x,t)$.

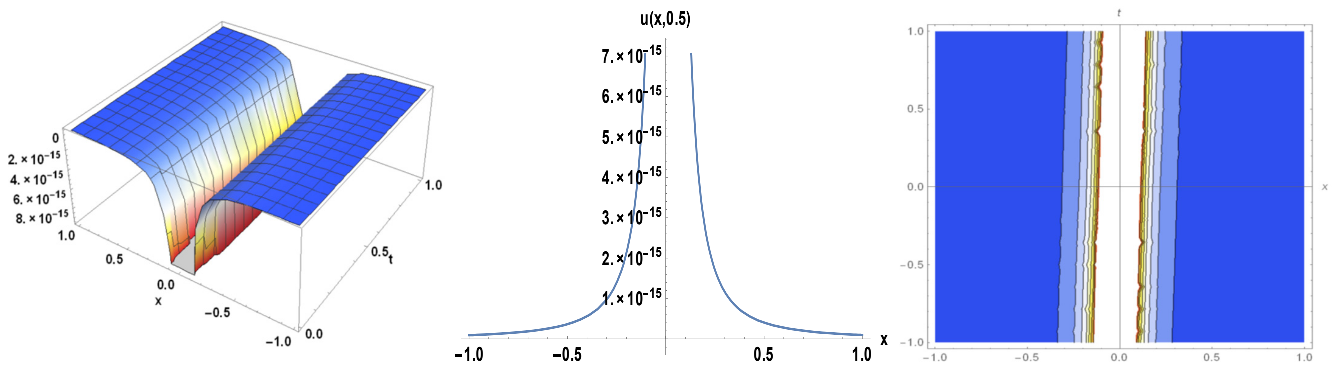

Figure 8. The solitary wave perspective view of the 3D, 2D and contour plots of $U_{10}(x,t)$.

5. Conclusions

By modelling soliton-like signals in microtubules as nonlinear RLC transmission lines, we were able to do analytical and numerical research on their propagation. These models are based on the structure of microtubule proteins. New analytical solutions, such as the solitary wave solutions depicted in Figures 1–8, were made possible by the modified exp-function approach. Here, we have considered only one case for the values of the positive integers $M = 3$ for $N = 1$. If we consider $M = 4$ for $N = 2$, then we can get more general solutions, which shows the novelty of our work. All the exact solutions attained in this article have been checked by using Maple 18 to the RLC transmission line model and found correct. This method has given numerous coefficients for Equations (15) and (16). This method proved useful for generating new analytical solutions to the solitary wave solutions exposed in Figures 1–8. It has been shown that the applied method is effective because it provides a lot of new solutions. We have also plotted 3D, 2D and contour graphs of the obtained solutions. We found trigonometric, hyperbolic, exponential, and rational function solutions in this study. The solutions obtained by Alam and Alam [18] are re-derived when parameters are given some specific values.

Author Contributions: Conceptualization, M.S.; Formal analysis, A.; Funding acquisition, J.D.C.; Investigation, A.; Resources, N.A.S.; Software, N.A.S.; Writing—original draft, M.S.; Writing—review & editing, J.D.C. All authors have read and agreed to the published version of the manuscript.

Funding: This work was supported by Korea Institute of Energy Technology Evaluation and Planning (KETEP) grant funded by the Korea government (MOTIE) (20202020900060, The Development and Application of Operational Technology in Smart Farm Utilizing Waste Heat from Particulates Reduced Smokestack).

Institutional Review Board Statement: Not applicable.

Informed Consent Statement: Not applicable.

Data Availability Statement: Not applicable.

Conflicts of Interest: The authors declare no conflict of interest.

References

1. Jawad, J.M.; Petković, M.D.; Biswas, A. Soliton solutions of a few nonlinear wave equations. *Appl. Math. Comput.* **2010**, *216*, 2649–2658.
2. Jafar, B.; Asadi, M.A.; Salehi, F. Rational Homotopy Perturbation Method for solving stiff systems of ordinary differential equations. *Appl. Math. Model.* **2015**, *39*, 1291–1299.
3. Cariello, F.; Tabor, M. Painlevé expansions for nonintegrable evolution equations. *Phys. D Nonlinear Phenom.* **1989**, *39*, 77–94. [CrossRef]
4. Philip, D.G.; Drazin, P.G.; Johnson, R.S. *Solitons: An Introduction*; Cambridge University Press: Cambridge, UK, 1989; Volume 2.
5. Aslam, M.N.; Akbar, M.A.; Mohyud-Din, S.T. General traveling wave solutions of the strain wave equation in microstructured solids via the new approach of generalized (G′/G)-expansion method. *Alex. Eng. J.* **2014**, *53*, 233–241. [CrossRef]
6. Shakeel, M.; Ul-Hassan, Q.M.; Ahmad, J.; Naqvi, T. Exact solutions of the time fractional BBM-Burger equation by novel (G'/G)-expansion method. *Adv. Math. Phys.* **2014**, *2014*, 181594. [CrossRef]
7. Zhou, Y.; Wang, M.; Wang, Y. Periodic wave solutions to a coupled KdV equations with variable coefficients. *Phys. Lett. A* **2003**, *308*, 31–36. [CrossRef]
8. Ali, A.T. New generalized Jacobi elliptic function rational expansion method. *J. Comput. Appl. Math.* **2011**, *235*, 4117–4127. [CrossRef]
9. Lü, D. Jacobi elliptic function solutions for two variant Boussinesq equations. *Chaos Solitons Fractals* **2005**, *24*, 1373–1385. [CrossRef]
10. Liu, S.; Fu, Z.; Liu, S.; Zhao, Q. Jacobi elliptic function expansion method and periodic wave solutions of nonlinear wave equations. *Phys. Lett. A* **2001**, *289*, 69–74. [CrossRef]
11. Fan, E. Two new applications of the homogeneous balance method. *Phys. Lett. A* **2000**, *265*, 353–357. [CrossRef]
12. Fan, E. Extended tanh-function method and its applications to nonlinear equations. *Phys. Lett. A* **2000**, *277*, 212–218. [CrossRef]
13. Sekulić, D.L.; Satarić, M.V.; Živanov, M.B. Symbolic computation of some new nonlinear partial differential equations of nanobiosciences using modified extended tanh-function method. *Appl. Math. Comput.* **2011**, *218*, 3499–3506. [CrossRef]
14. Soliman, A.A. The modified extended tanh-function method for solving Burgers-type equations. *Phys. A Stat. Mech. Its Appl.* **2006**, *361*, 394–404. [CrossRef]
15. Li, Z.; Liu, Y. RATH: A Maple package for finding travelling solitary wave solutions to nonlinear evolution equations. *Comput. Phys. Commun.* **2002**, *148*, 256–266. [CrossRef]
16. Peng, Y.Z. A mapping method for obtaining exact travelling wave solutions to nonlinear evolution equations. *Chin. J. Phys.* **2003**, *41*, 103–110.
17. Yomba, E. Construction of new soliton-like solutions of the (2 + 1) dimensional dispersive long wave equation. *Chaos Solitons Fractals* **2004**, *20*, 1135–1139. [CrossRef]
18. Alam, N.; Alam, M.M. An analytical method for solving exact solutions of a nonlinear evolution equation describing the dynamics of ionic currents along microtubules. *J. Taibah Univ. Sci.* **2017**, *11*, 939–948. [CrossRef]
19. Jeffrey, A.; Mohamad, M.N.B. Exact solutions to the KdV-Burgers' equation. *Wave Motion* **1991**, *14*, 369–375. [CrossRef]
20. Jawad, A.J.M.; Petković, M.D.; Biswas, A. Soliton solutions of Burgers equations and perturbed Burgers equation. *Appl. Math. Comput.* **2010**, *216*, 3370–3377.
21. Satarić, M.V.; Ilić, D.I.; Ralević, N.; Tuszynski, J.A. A nonlinear model of ionic wave propagation along microtubules. *Eur. Biophys. J.* **2009**, *38*, 637–647. [CrossRef]
22. Satarić, M.V.; Sekulić, D.; Živanov, M. Solitonic ionic currents along microtubules. *J. Comput. Theor. Nanosci.* **2010**, *7*, 2281–2290. [CrossRef]

23. Sekulić, D.L.; Satarić, B.M.; Tuszynski, J.A.; Satarić, M.V. Nonlinear ionic pulses along microtubules. *Eur. Phys. J. E* **2011**, *34*, 49. [CrossRef] [PubMed]
24. Zayed, E.M.E.; Amer, Y.A.; Shohib, R.M.A. The improved generalized Riccati equation mapping method and its application for solving a nonlinear partial differential equation (PDE) describing the dynamics of ionic currents along microtubules. *Sci. Res. Essays* **2014**, *9*, 238–248.
25. Shakeel, M.; Iqbal, M.A.; Din, Q.; Hassan, Q.M.; Ayub, K. New exact solutions for coupled nonlinear system of ion sound and Langmuir waves. *Indian J. Phys.* **2020**, *94*, 885–894. [CrossRef]